

Calibration-Free Evapotranspiration Mapping (CREMAP) results for the High Plains aquifer, USA

Jozsef Szilagyi
Conservation and Survey Division
School of Natural Resources
University of Nebraska-Lincoln

Methodology

The complementary relationship (CR) of evaporation, originally proposed by Bouchet (1963), was subsequently formulated for practical regional-scale ET applications by Brutsaert & Stricker (1979) and Morton et al. (1985). In this study the WREVAP program of Morton et al. (1985) was applied for the estimation of the regional-scale ET rates at monthly periods. Disaggregation of the regional ET value in space is based on the Moderate Resolution Imaging Spectroradiometer (MODIS) data (NASA, 2012) that have a nominal spatial resolution of about 1 km. The disaggregation is achieved by a linear transformation of the 8-day composited MODIS daytime surface temperature (T_s) values into actual ET rates on a monthly basis (Szilagyi et al., 2011; Szilagyi and Jozsa, 2009) by first aggregating the composited T_s data into monthly mean values. Compositing is used for eliminating cloud effects in the resulting composite data by removing suspicious, low pixel-values in the averaging over each eight-day period. See (NASA, 2012) for more detail of data collection and characteristics.

The transformation requires the specification of two anchor points in the T_s versus ET plane (Figure 1). The first anchor point is defined by the spatially averaged daytime surface temperature, $\langle T_s \rangle$, and the corresponding regionally representative ET rate, E , from WREVAP. (The original FORTRAN source code can be downloaded from the personal website of the author: snr.unl.edu/~szilagyi/szilagyi.htm). The second anchor point comes from the surface temperature, T_{sw} , of a completely wet cell and the corresponding wet-environment evaporation, E_w , [defined by the Priestley-Taylor (1972) equation with a coefficient value of 1.2]. The two points identify the linear transformations of the T_s pixel values into ET rates for each month. The resulting line is extended to the right, since in about half the number of the pixels ET is less than the regional mean, E . A monthly time-step is ideal because most of the watershed- or large-scale hydrologic models work at this time-resolution, plus a monthly averaging further reduces any lingering cloud effect in the 8-day composited T_s values. Wet cells within the region were identified over a) Lake McConaughy and the Lewis and Clark Lake on the Missouri River in Nebraska; b) Glendo reservoir in Wyoming; c) Cheney reservoir in Kansas, and; d) Foss reservoir in Oklahoma. (Most reservoirs do not have a large enough surface area to eliminate “land contamination” problems in the T_s values). An inverse-distance weighting method was subsequently used to calculate the T_{sw} value to be assigned to a given MODIS cell for the linear transformation.

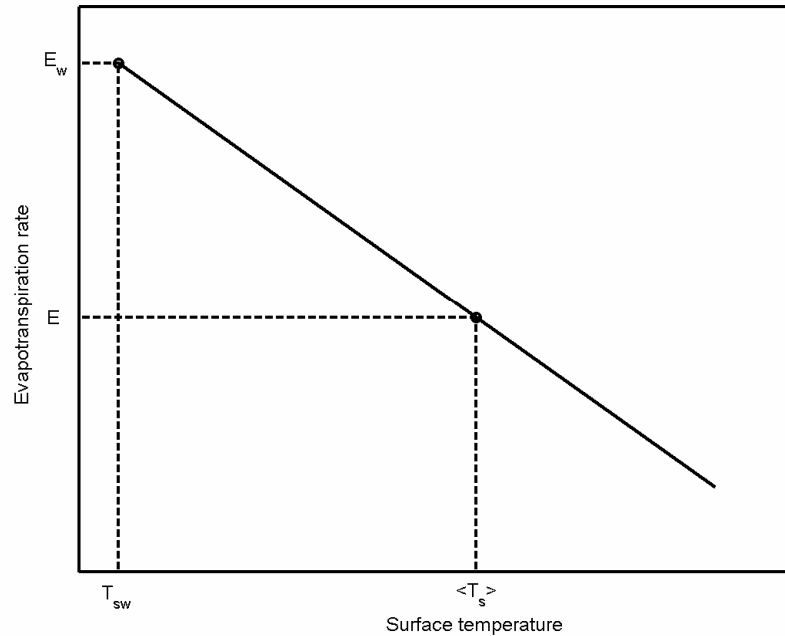


Fig. 1. Schematics of the linear transformation of the MODIS daytime surface temperature values into ET rates (after Szilagyi et al., 2011), applied in CREMAP.

The core assumption of CREMAP is that the surface temperature of any MODIS cell is predominantly defined by the rate of evapotranspiration due to the large value of the latent heat of vaporization for water and that the energy (Q_n) available at the surface for sensible (i.e., heat convection) and latent heat (i.e., evapotranspiration) transfers are roughly even among the cells of a flat-to-rolling terrain. Heat conduction into the soil is typically negligible over a 24-hour period, and here considered negligible over the daytime hours as well. This last assumption is most likely true for fully vegetated surfaces where soil heat conduction is small throughout the day, and is less valid for bare soil and open water surfaces. While a spatially constant Q_n term at first seems to be an overly stringent requirement in practical applications due to spatial changes in vegetation cover as well as slope and aspect of the land surface, Q_n will change only negligibly in space provided the surface albedo (i.e., the ratio of in- and outgoing short-wave radiation) value also changes negligibly among the pixels over a flat or rolling terrain. For the study region, the MODIS pixel size of about 1 km may indeed ensure a largely constant Q_n value among the pixels since e.g., the observed standard deviation in the mean monthly (warm season) surface albedo value of 17% was only 1.2% among the MODIS cells in Nebraska (Szilagyi, 2013).

A further assumption of the method is that the vertical gradient of the air temperature near the surface is linearly related to the surface temperature (Bastiaanssen et al., 1998; Allen et al., 2007), thus sensible heat (H) transfer across the land-atmosphere interface, provided changes in the aerodynamic resistance (r_a) among the MODIS pixels are moderate, can also be taken a linear function of T_s . This can be so because under neutral atmospheric conditions (attained for time-steps a day or longer) r_a depends linearly on the logarithm of the momentum roughness length, z_{0m} (Allen et al., 2007), thus any change in z_{0m} between pixels becomes significantly dampened in the r_a value due to the logarithm. Consequently, the latent heat (LE) transfer itself becomes a linear function of T_s under a spatially constant net energy (Q_n) term required by the CR, therefore $Q_n = H + LE$, from which $LE = mT_s + c$ follows, m and c being constants for the computational time step, i.e., a month here, within a region.

8-day composited MODIS daytime surface temperature data were collected over the 2000 – 2009 period. The 8-day composited pixel values were averaged for each month to obtain one surface temperature per pixel per month, except for December, January, and February. The winter months were left out of the linear transformations because then the ground may have patchy snow cover which violates the constant Q_n assumption since the albedo of snow is markedly different from that of the land. Therefore in the wintertime the WREVAP-derived regional ET rates were employed without any further disaggregation by surface temperatures but, rather, with a subsequent correction, discussed in Szilagyi (2013).

Mean annual precipitation (Figure 3), mean monthly maximum/minimum air and dew-point temperature values came from the PRISM database (Daly et al., 1994) at 2.5-min spatial resolution. Mean monthly incident global radiation data at half-degree resolution were downloaded from the GCIP/SRB site (GEWEX, 2012). While previously (Szilagyi et al., 2011) the regions were defined by subdividing the study area into distinct areas (a largely arbitrary process) for the calculation of the regionally representative values of the mean monthly air temperature, humidity and radiation data, required by WREVAP, now such a subdivision is not necessary. Instead, a “radius of influence” is defined over which the regional values are calculated separately for each designated MODIS cell, very similar to a temporal moving-average process, but now in two dimensions of space. In principle, such a spatial averaging could be performed for each MODIS cell, in practice however, it becomes computationally overwhelming on the PC, and it is also unnecessary, since the spatial averages form a 2-D signal of small gradient, making possible that “sampling” (i.e., the actual calculation of the spatial mean values including the WREVAP-calculated ET rate) is performed only in a selected set of points, which was chosen as each tenth MODIS cell in space (both row-, and column-wise). The remaining cells were then filled up with spatial mean values, linearly interpolated first by row among the selected MODIS-cell values, and then by column, involving the already interpolated values in the rows as well. This “sampling” sped up calculations by at least two orders of magnitude.



Fig. 2. Extent of the High Plains aquifer within the US with a 35-km buffer zone employed for spatial averaging.

Care had to be exercised with the choice of the radius of influence. Two values were chosen, 100 and 50 km, and the latter was kept eventually due to its slightly better performance with catchment water-balance data. It was simpler to define a rectangular region around each designated MODIS cell, rather than a circular one, therefore the radius of influence is half the side-length of the resulting square. It was possible to apply a constant radius value,

because of the ca. 35-km buffer zone employed around the study region (Figure 2). Without such a buffer zone the radius should have been reduced in the vicinity of the borders (see Szilagyi, 2013) in order to avoid asymmetrical averaging.

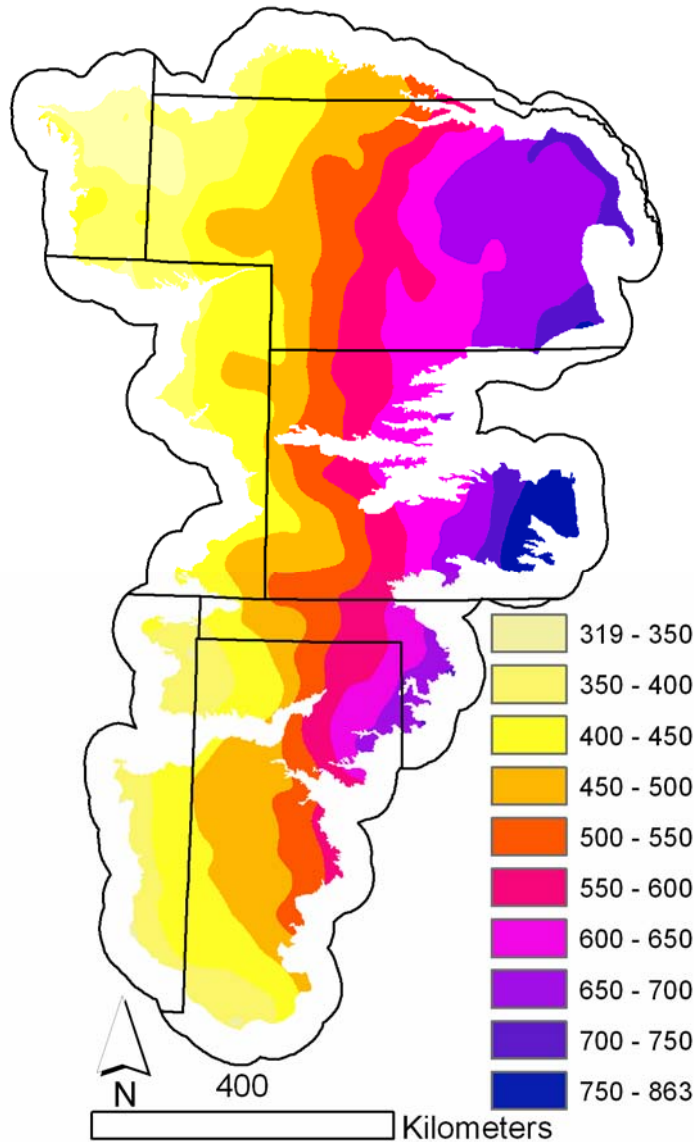


Fig. 3. Spatially smoothed mean (2000-2009) annual PRISM precipitation (mm). Regional average is 516 mm.

Once the spatial mean values were available for each MODIS cell, the actual linear transformation of the T_s to ET values was performed for each month (except the winter months). The linear transformation of the T_s values into ET rates assumes a negligible change in the r_a value among the cells. As was mentioned above, r_a is directly proportional –up to a constant and with a negative slope— to the logarithm of z_{0m} under neutral stability conditions of the atmosphere, provided the wind speed at the blending height (about 200 m above the ground) is near constant within the region (Allen et al., 2007). The momentum roughness height, z_{0m} , of each MODIS cell has been estimated over the region (Figure 4a) with the help of a 1-km digital elevation model, as the natural logarithm of the standard deviation in the elevation values among the 25 neighboring cells surrounding a given cell, including the chosen cell itself. The minimum value of z_{0m} has been set to 0.4 m, so when the estimate

became smaller than this lower limit (possible for flat regions), the value was replaced by 0.4 m. Note that the $z_{0m} = 0.4$ m value is the upper interval value for a “prairie or short crops with scattered bushes and tree clumps” in Table 2.6 of Brutsaert (2005). The rugged hills regions of Nebraska (e.g., the Pine Ridge and the Pine Bluffs, just to name a few) are characterized (Figure 2) by the largest z_{0m} values (larger than 3 m), covering the 3-4 m range for “Fore-Alpine terrain (200-300 m) with scattered tree stands” of Brutsaert (2005). Since the r_a estimates are proportional (up to a constant) to the logarithm of the z_{0m} values, their change among the MODIS cells is much subdued (Figure 4b): about 67% of the time they were within 5% of their spatial mean and more than 94% of the time they remained within 15% in Nebraska (Szilagyi, 2013), supporting the original assumption of the present ET mapping method.

Cells that had r_a values smaller than 95% of the mean r_a value were identified, and the corresponding ET values corrected by the relative change in r_a , considering that the sum of the latent (LE) and sensible heat (H) values are assumed to be constant among the cells (equaling Q_n) and that H is proportional to dT_z / r_a (Allen et al., 2011), where dT_z is the vertical gradient of the air temperature above the surface, itself taken proportional to T_s . The reason that only the “overestimates” of ET are corrected is that the linear transformation of the T_s values into ET rates seems to be more sensitive to more rugged-than-average terrain than to smoother one. Clearly, over smooth terrain the vegetation exerts a more pronounced effect on the z_{0m} value than over rugged one. Additional adjustments for Nebraska were the same as in Szilagyi (2013). A final correction was applied for cells of “extreme” elevation. Namely, when the elevation of a cell differed from the regional mean value by more than 100 m, its surface temperature was corrected by 0.01 Kelvin per meter, reflecting the dry-adiabatic cooling rate of the air.

The WREVP model is based on the complementary relationship which performs the worst in the cold winter months (Szilagyi and Jozsa, 2009; Huntington et al., 2011; Szilagyi et al., 2009), thus the resulting WREVP-obtained winter ET rates become the most uncertain. WREVP winter months were fully included in the mean annual ET rates for areas where the mean monthly daytime maximum temperature values exceeded 5 °C. This line cuts across Nebraska. See Szilagyi (2013) for winter-time adjustments within Nebraska.

Results and discussion

The mean annual ET rates across the High Plains aquifer are displayed in Figure 5. The values are corrected values because it was observed that the CR underestimated the regional ET rates around the south-western edge of the region due to significant summer heat advection from the semi-arid regions of Colorado and New Mexico (identified by decreasing precipitation rates across the western border of the study area). The correction involved dividing the WREVP ET value by the ratio of its value and the corresponding precipitation (P) rate whenever the WREVP ET rate was smaller than 95% of P and the spatially smoothed mean annual precipitation rate was smaller than 450 mm. The 95% was chosen, because the runoff ratio [obtained from computed runoff data of USGS (2012) HUC8-level watersheds] in this region is smaller than 5% of P.

The regional average of 490 mm/yr is close to the USGS-published (2011) value of 472 mm by the Simplified Surface Energy Balance (SSEB) model of Senay et al. (2007, 2011). The two ET estimation methods are similar: they both use a linear transformation of the MODIS surface temperatures (T_s). While SSEB uses the T_s values of two extremes: the wet and completely dry cells, CREMAP uses the average T_s of the region for the latter, which is arguably more readily and more accurately obtainable than the often non-existent completely dry cell surface temperature.

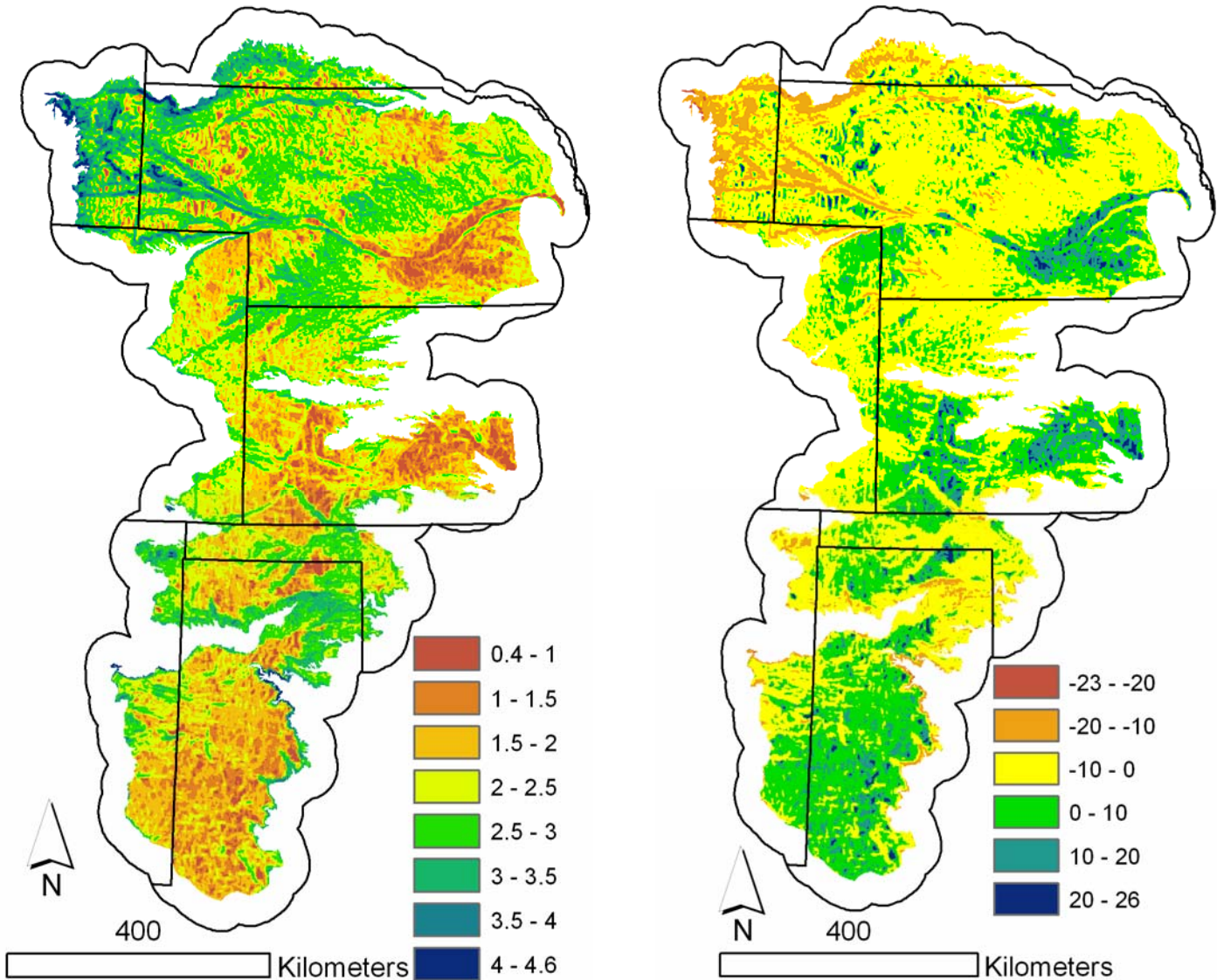


Fig. 4. Estimated values of the a) momentum roughness height (m), and; b) relative change (%) in aerodynamic resistance around its spatial mean value.

The regional average of 95% for the precipitation recycling ratio is identical to the one obtained for Nebraska by Szilagyi (2013). Note that it does not mean that only 5% of the precipitation contributes to runoff on average. The actual runoff contribution is somewhat larger because some of the ET originates from reductions in groundwater levels. For the transformation of observed groundwater level changes into actual water depth, one would need a map of the specific yield values across the study area. This author is not aware of such a regional-scale map. The effect of large-scale irrigation is clearly visible in Figure 5b, with ET rates often exceeding (purple to blue colors) the precipitation rates.

Figure 6 displays the USGS HUC8-level watershed-scale errors [estimated minus observed (the latter obtained as P less USGS computed runoff)] in the mapped ET rates. The estimates are within 15% of the water-balance derived values. In Figure 7 the resulting linear correlation is shown between the two types of ET values with an explained variance of 85%. The top and bottom lines designate the water-balance derived value plus/minus 10%.

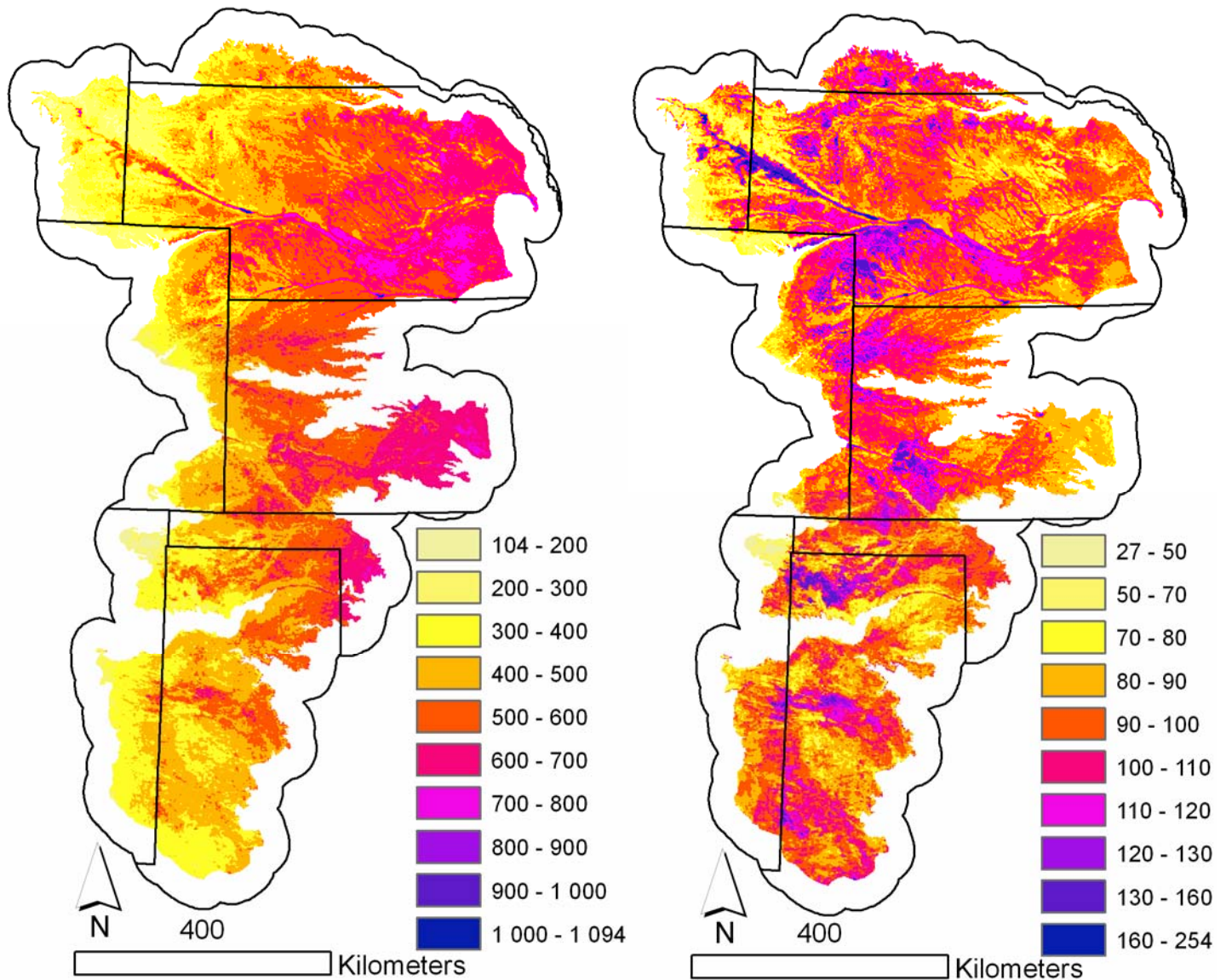


Fig. 5. Mean annual (2000-2009) ET rates (mm) and ET / P ratios (%) over the High Plains aquifer. The spatial averages are 490 mm and 95%, respectively.

The arithmetic (non-area weighted) averages of the 95 values of Figure 7 are 519 and 514 mm for the water-balance and CREMAP ET rates, while the regional averages (i.e., area-weighted) are 497 and 490 mm, respectively.

Acknowledgments: This work has been supported by the Agricultural Research Division of the University of Nebraska.

Disclaimer: The views, conclusions, and opinions expressed in this study are solely those of the writer and not the University of Nebraska, state of Nebraska, or any political subdivision thereof.

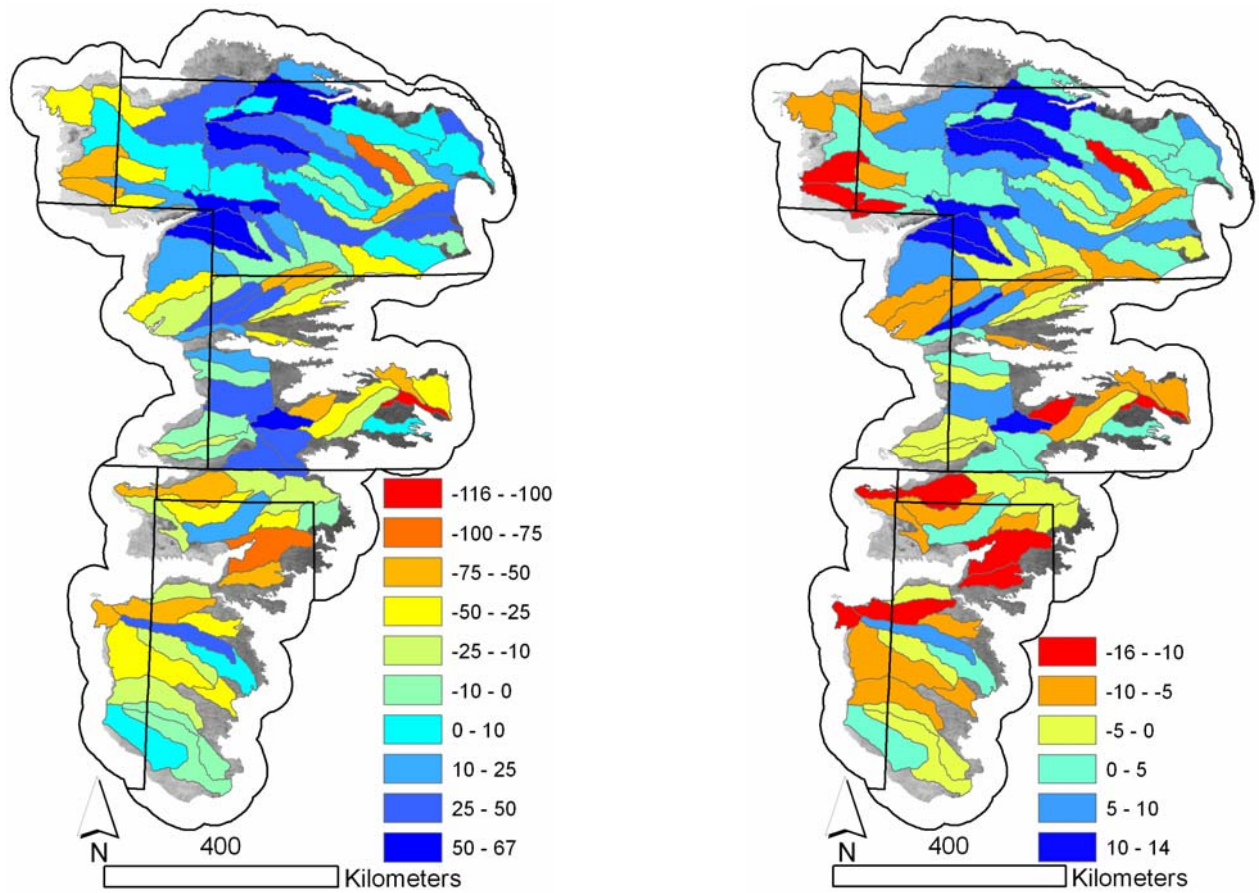


Fig. 6. Absolute (mm) and relative errors (%) in the USGS HUC8-level watershed representative mean annual ET estimates.

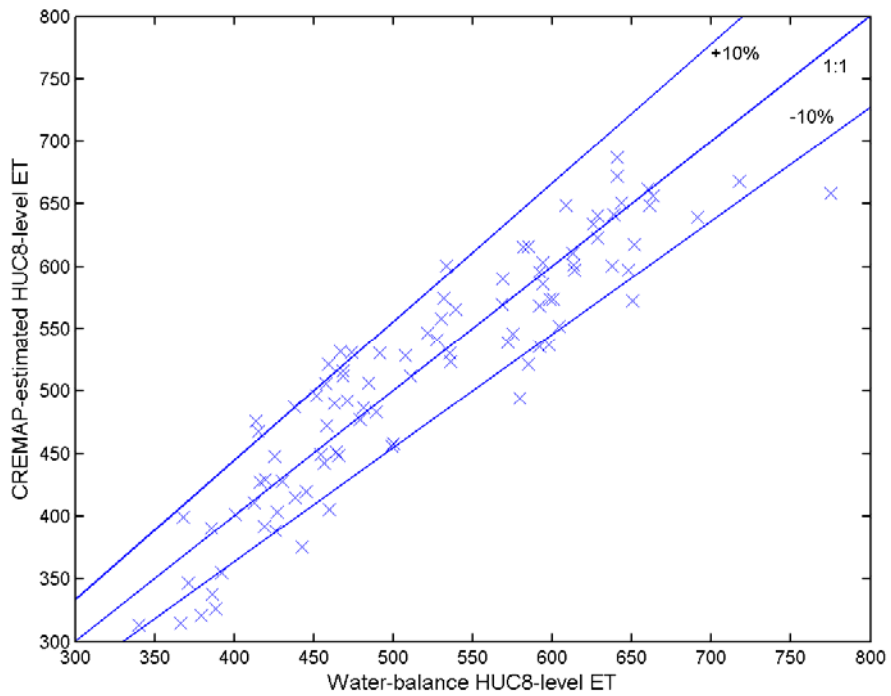


Fig. 7. “Observed” vs estimated HUC8-level mean (2000-2009) annual ET rates (mm). $R^2=85\%$.

REFERENCES

- Allen R., Tasumi M., Trezza R., 2007. Satellite-based energy balance for mapping evapotranspiration with internalized calibration (METRIC)-model. *Journal of Irrigation and Drainage Engineering*, 133(4), 380-394.
- Bastiaanssen W., Menenti M., Feddes R., Holtslag A., 1998. A remote sensing surface energy balance algorithm for land (SEBAL): 1. Formulation. *Journal of Hydrology*, 212, 198–212.
- Bouchet, R. J., 1963. Evapotranspiration reelle, evapotranspiration potentielle, et production agricole. *Annales Agronomique*, 14, 543–824.
- Brutsaert W., 2005. *Hydrology: An Introduction*. Cambridge University Press, Cambridge, United Kingdom.
- Brutsaert W., Stricker H., 1979. An Advection–Aridity approach to estimate actual regional evapotranspiration. *Water Resources Research*, 15, 443–449.
- Daly C., Neilson R. P., Phillips D. L., 1994. A statistical-topographic model for mapping climatological precipitation over mountainous terrain. *Journal of Applied Meteorology*, 33, 140-158. Available from www.prism.oregonstate.edu (accessed 28 June 2012).
- GEWEX Continental Scale International Project, Surface Radiation Budget, GCIP-SRB. <http://metosrv2.umd.edu/~srb/gcip/cgi-bin/historic.cgi> (accessed 28 June 2012).
- Huntington J., Szilagyi J., Tyler S., Pohl G., 2011. Evaluating the Complementary Relationship for estimating evapotranspiration from arid shrublands. *Water Resources Research*, 47, W05533.
- Morton F., Ricard F., Fogarasi S., 1985. Operational estimates of areal evapotranspiration and lake evaporation – Program WREVAP. National Hydrological Research Institute (Ottawa, Canada) Paper 24.
- National Aeronautics and Space Administration. Moderate Resolution Imaging Spectroradiometer, MODIS data. <http://modis.gsfc.nasa.gov> (accessed 28 June 2012).
- Priestley C., Taylor R., 1972. On the assessment of surface heat flux and evaporation using large-scale parameters. *Monthly Weather Review*, 100, 81–92.
- Senay, G.B., Budde, M.E., Verdin, J.P., Melesse, A.M., 2007. A coupled remote sensing and simplified surface energy balance approach to estimate actual evapotranspiration from irrigated fields. *Sensors*, 7, 979–1000.
- Senay, G.B., Budde, M.E., Verdin, J.P., 2011. Enhancing the simplified surface energy balance (SSEB) approach for estimating landscape ET—Validation with the METRIC model. *Agricultural Water Management*, 98(4), 606–618.
- Szilagyi J., Kovacs A., Jozsa J., 2011. A calibration-free evapotranspiration mapping (CREMAP) technique. In: Labeledzki L. (ed.) *Evapotranspiration*. Rijeka: InTech, 257-274. Available from <http://www.intechopen.com/books/show/title/evapotranspiration> (accessed 28 June 2012).

Szilagyi J., Jozsa J., 2009. Estimating spatially distributed monthly evapotranspiration rates by linear transformations of MODIS daytime land surface temperature data. *Hydrology and Earth System Science*, 13(5), 629-637.

Szilagyi J., Hobbins M., Jozsa J., 2009. A modified Advection-Aridity model of evapotranspiration. *Journal of Hydrologic Engineering*, 14(6), 569-574.

Szilagyi, J., 2013. Recent Updates of the Calibration-Free Evapotranspiration Mapping (CREMAP) Method. In: Grgur D. (ed.) *Evapotranspiration – An Overview*. Rijeka: InTech, ISBN 980-953-307-541-4, in press.

United States Geological Survey, 2011. Selected approaches to estimate water-budget components of the High Plains, 1940 through 1949 and 2000 through 2009. SIR 2011-5183.